

# Observation of corona discharges and cloud microphysics at the top of thunderstorm cells in cyclone Fani

Dongshuai Li<sup>1</sup>, Torsten Neubert<sup>1</sup>, Lasse Skaaning Husbjerg<sup>1</sup>, Yanan Zhu<sup>2</sup>,  
Olivier Chanrion<sup>1</sup>, Jeff Lapierre<sup>2</sup>, Alejandro Luque<sup>3</sup>, Christoph Köhn<sup>1</sup>,  
Matthias Heumesser<sup>1</sup>, Krystallia Dimitriadou<sup>1</sup>, Martin Stendel<sup>4</sup>, Eigil Kaas<sup>4,5</sup>,  
Emilie Petrea Petajamaa Wiinberg Olesen<sup>1</sup>, Feifan Liu<sup>6</sup>, Nikolai Østgaard<sup>7</sup>, Víctor Reglero<sup>8</sup>

<sup>1</sup>National Space Institute, Technical University of Denmark (DTU Space), Kongens Lyngby, Denmark.

<sup>2</sup>Earth Networks, Germantown, MD, USA.

<sup>3</sup>Instituto de Astrofísica de Andalucía (IAA), CSIC, Granada, Spain.

<sup>4</sup>Danish Meteorological Institute, Copenhagen, Denmark.

<sup>5</sup>University of Copenhagen, Niels Bohr Institute, København K, Denmark.

<sup>6</sup>CAS Key Laboratory of Geospace Environment, University of Science and Technology of China, Hefei, China.

<sup>7</sup>Birkeland Centre for Space Science, Department of Physics and Technology, University of Bergen, Bergen, Norway.

<sup>8</sup>Image Processing Laboratory, University of Valencia, Valencia, Spain.

## Key Points:

- We present the first observations of blue corona discharges associated with a tropical cyclone.
- The microphysical parameters related to the corona discharges are measured almost simultaneously by the CALIPSO satellite.
- The discharges are associated with strong convection with relatively high ice content at the cloud tops.

---

Corresponding author: Dongshuai Li, National Space Institute, Technical University of Denmark (DTU Space), Kongens Lyngby, Denmark, dongshuai@space.dtu.dk

## Abstract

Blue corona discharges are bursts of streamers often observed at the top of thunderclouds, but the cloud conditions that facilitate them are not well known. Here we present observations by the Atmosphere-Space Interactions Monitor of 92 corona discharges as it passed over cyclone Fani in the Bay of Bengal. The discharges formed in convective cells of unstable air carried from land over the Indian Ocean, with CAPE reaching  $\sim 6000 \text{ J kg}^{-1}$ . The CALIPSO satellite passed over one of the cells  $\sim 12$  min after ASIM, taking the first measurements of the microphysics at the top of a cloud generating corona discharges. We find the discharges occur in a region of strong convection, the cloud reaching into the stratosphere with ice/water content  $\sim 0.1 \text{ g m}^{-3}$ , photon mean free path  $\sim 3 \text{ m}$  and ice crystal number density  $\sim 5 \times 10^7 \text{ m}^{-3}$ . Measurements by a lightning detection network suggest the charge structures are folded.

## Plain Language Summary

Blue corona discharges are bursts of streamers that often are observed at the top of thunderclouds, but the conditions in the clouds that generate them are not well understood. In this study, we discuss observations of corona discharges in convective cells detected by ASIM on the International Space Station as it passed over cyclone Fani in the Bay of Bengal. For the first time, we have observations of the cloud particle characteristics at the cloud tops taken shortly afterward by the CALIPSO satellite. The observations indicate that the corona discharges are associated with strong convection in cloud cells that reach into the stratosphere. The cloud parameters are important for theoretical studies of the discharge conditions.

## 1 Introduction

The lightning leader, as the bright luminous channel of lightning, is a highly ionized plasma with the high temperature which can lead to the dissociation of a significant amount of molecular oxygen into atomic oxygen. A lightning channel has therefore high electrical conductivity and is often detected by optical means at the atomic line of OI line in  $777.4 \text{ nm}$  (Christian et al., 1989; Blakeslee et al., 2020; Goodman et al., 2013; Grandell et al., 2010; Yang et al., 2017). Streamers are waves of ionization that create filaments of low-density, cold plasma with no atomic oxygen (Ebert & Sentman, 2008). Bursts of streamers may be generated without a leader, may initiate a leader, or may be formed in the high electric field region ahead of a leader tip forming a streamer corona (da Silva & Pasko, 2013). In the atmosphere, at altitudes up to  $\sim 50 \text{ km}$ , they appear blue with strong emissions at  $337 \text{ nm}$  of  $\text{N}_2^2\text{P}$  in the near-ultra violet band (Raizer & Allen, 1991; Montanyà et al., 2021; Walker & Christian, 2019; Chanrion et al., 2019; Gordillo-Vázquez & Pérez-Invernón, 2021).

Blue corona discharges within the clouds or close to the top of clouds are difficult to observe because of light scattering in the cloud. If they rise above the clouds into the stratosphere, they are more readily observed and have been given names such as *blue starters* and *gnomes* that reach a few km above the clouds, *blue jets* that may reach the stratopause, and *gigantic jets* from cloud tops to the ionosphere where the lower portion in the stratosphere is blue. It is debated to what extent these types of discharges are of streamer and/or leader nature (Wescott et al., 1996, 2001; Lyons et al., 2003; Pasko, 2008; Neubert et al., 2021; Gordillo-Vázquez & Pérez-Invernón, 2021).

Corona discharges within or near cloud tops were observed by The Imager of Sprites and Upper Atmospheric Lightning (ISUAL) instruments on FormoSat-2 (F. Liu et al., 2018; Chou et al., 2018) and from the ISS at a rate of about 120 per minute (Chanrion et al., 2017). In 2018, the Atmosphere-Space Interactions Monitor (ASIM) was installed on the International Space Station (ISS) with instruments designed to measure lightning processes (Neubert et al., 2019). With ASIM measurements, corona discharges were found to be common with a global total rate of about  $11 \text{ s}^{-1} \text{ km}^{-2}$  at local midnight (Soler et al., 2021). The optical rise times of the discharges falls in two categories: one with fast rise times  $\leq 30 \mu\text{s}$  (fast discharges) and another with longer rise times (slow discharges) (Husbjerg et al., 2022). The rise times reflect the amount of photon scattering by

cloud hydrometeors and are therefore a measure of the depth in the cloud of the discharge (Luque et al., 2020).

There is a growing amount of studies on corona discharges based on ASIM measurements (Soler et al., 2020, 2021; Li et al., 2021; Li, Luque, Lehtinen, et al., 2022; Dimitriadou et al., 2022; Husbjerg et al., 2022; F. Liu, Lu, et al., 2021). We know that such discharges are favoured by stronger convection and higher cloud tops than normal lightning (Husbjerg et al., 2022) and occur in cells that are under development (Dimitriadou et al., 2022). However, the conditions in the clouds that generate them are still not well understood.

Recent studies have linked corona discharges with a special type of intra-cloud discharge named Narrow Bipolar Events (NBEs) (Soler et al., 2020; F. Liu, Lu, et al., 2021; Li et al., 2021; Li, Luque, Lehtinen, et al., 2022; F. Liu et al., 2018; F. Liu, Zhu, et al., 2021; Chou et al., 2018). NBEs are short (10-20  $\mu$ s) and Very High Frequency (VHF) (hundreds of MHz) radio signals emitted from thunderstorms (Smith et al., 1999, 2004; Wu et al., 2012), which are likely produced by electrical discharges named Fast Breakdowns (FBs). They may contribute in the initial stage of lightning flashes (Rison et al., 2016; N. Liu et al., 2019; Tilles et al., 2019; Li, Luque, Gordillo-Vázquez, et al., 2022) or blue jets (Neubert et al., 2021). Whereas measurements from ASIM give a snapshot of the discharge occurrences as the ISS passes overhead, ground based measurements of lightning and NBEs give a larger context for analysis.

In this study, 92 corona discharges are detected by ASIM as it passes over the cyclone Fani in the Bay of Bengal. We present the first combined observation of corona discharges from ASIM and cloud properties by the Cloud-Aerosol Lidar and Infrared Pathfinder Satellite Observation (CALIPSO) that passed over a thunderstorm cell about 12 minutes after ASIM. Using the data of CALIPSO, we analyze the detailed cloud microphysical features related to the corona discharges and investigate their correlation with NBEs and lightning in the convective cells forming in a tropical cyclone, measured by a ground-based lightning detection system.

## 2 Instruments and Observations

On April 26, 2019, a tropical depression in the southern region of the Bay of Bengal deepened into cyclone Fani. As Fani moved northward, it developed into a category 4 cyclone on May 2 with wind speeds of up to 250 km per hour. It was the most severe cyclone in the Bay of Bengal since 1999, killing 81 people and causing damages of approximately 8.1 billion US dollars at landfall in Bangladesh and India (Zhao et al., 2020; Chauhan et al., 2021).

ASIM passed over Fani on April 30, 2019, when it was a category 3 cyclone. Its nadir-pointing instruments include three photometers that sample at 100 kHz and two cameras that image at 12 frames per second. The photometers measure part of the Lyman–Birge–Hopfield (LBH) band of  $N_2$  in the ultraviolet (UV) band at 180 - 230 nm, the second positive line of  $N_2$  at 337 nm (blue) with 3 nm bandwidth and the atomic oxygen line OI at 777.4 nm (red) with 5 nm bandwidth. The cameras measure in the blue and red bands of the two photometers with a spatial resolution on the ground around 400 m  $\times$  400 m (Chanrion et al., 2019).

During its overpass from 20:10:55 to 20:12:05 UTC, ASIM detected 92 corona discharges from two convective cells  $\sim$  200 km from the cyclone center. The discharges had strong signals in the blue band with weak or absent emissions in the red, signifying faint or no associated leader activity, e.g., the marking of corona streamer discharges.

Figure 1(a) shows the cloud Top Blackbody Brightness (TBB) temperature derived from Himawari-8 satellite data (Bessho et al., 2016) at 20:10:00 UTC, with the location of the corona discharges estimated by projecting the camera measurements to 16 km altitude. The accuracy of the projection is better than 10 km (Neubert et al., 2021; Husbjerg et al., 2022). Also shown are the lightning flashes detected by the Earth Networks Total Lightning Network (ENTLN) during the overpass and the sites of the network sensors (Zhu et al., 2017, 2022). The ENTLN data were used to search for NBEs associated with corona discharges observed by ASIM and to characterize the electrical activity of the

storm cells. The time shift of ASIM is  $1.4 \pm 1$  ms, found by comparing to the measurements of the Lightning Imaging Sensor (LIS) on the ISS, similar to the study in Bitzer et al. (2021); Heumesser et al. (2021) (see Figure S1 in Supplemental Material).

In order to investigate CALIPSO observations around the area of corona activity, we define the region  $\beta$  (a rectangle of area  $50 \text{ km}^2$ ) shown in Figure 1(c), over which CALIPSO passed from 20:23:58 to 20:24:14 UTC. The measurements by its lidar give information on the microphysical and optical properties of the cloud cell with vertical distributions of hydrometeor properties (Z. Liu et al., 2009; Sourdeval et al., 2018; Gryspeerd et al., 2018; Delanoë & Hogan, 2010) within the 12 minutes after the observations by ASIM.

The meteorological context is illustrated in Figure 1(b), which shows the Convective Available Potential Energy (CAPE) from ERA5 hourly reanalysis data at 20:00:00 UTC. ERA5 provides hourly estimates of atmospheric, land and oceanic climate variables on a 30 km grid, and resolves the atmosphere using 137 levels from the surface to 80 km altitude (Hersbach et al., 2020). The corona discharges were generated under conditions with large CAPE values, reaching  $6000 \text{ J kg}^{-1}$  in region  $\beta$ . According to Husbjerg et al. (2022), it is one of the largest values associated with corona discharges during the past three years of ASIM observations. The cloud cells formed as air mass from mainland India carried by the cyclone winds out over the warm Bengal Ocean. The magnitude of 200 - 850 hPa vertical wind shear at the center of region  $\beta$  is  $\sim 20 \text{ m s}^{-1}$  (not shown here), common for severe convective storms (Pucik et al., 2021).

### 3 Analysis and Results

The CALIPSO lidar provides information on the vertical structure and properties of optically thin clouds and can detect small ice particle distributions on top of clouds that are generally missed by meteorological radars (Hagihara et al., 2014; Winker et al., 2010). Figure 2(a) shows a cross-section of the 532 nm lidar backscatter coefficient profile along the trajectory of CALIPSO in region  $\beta$ , and Figure 2(b) gives the Cloud Top Height (CTH) derived from these measurements. The tropopause height indicated by the black dashed line is obtained from the CALIPSO data product. It is provided by NASA's Global Modeling and Assimilation Office (GMAO) (*Lidar Level 1 V4.10 Data Product Descriptions*, 2016). The data are shown with time increasing along the  $x$ -axis, where the latitudes and longitudes are marked. For latitudes between  $11^\circ$ - $11.5^\circ$ , the main clouds reach 15-16 km altitude, increasing steeply to above 17 km at  $\sim 11.40^\circ$ ; this is likely where the main convection occurs. The cloud protrudes above the tropopause with layers reaching above the main clouds, the highest one with a gullwing-shaped cirrus layer of ice crystals pumped into the lower stratosphere (Wang et al., 2016; O'Neill et al., 2021) and carried from the region by wind shear near the cloud top.

Figures 2(c-f) show a selection of microphysical properties based on the raDAR/liDAR (DAR-DAR) cloud products (Delanoë & Hogan, 2010), namely the ice water content (c), categorization (d), photon mean free path (e) and ice crystal number density (f). These products are normally found with a variational method and, in the case of the ice crystal number density, by combining lidar and CloudSat radar measurements (Sourdeval et al., 2018; Gryspeerd et al., 2018; Delanoë & Hogan, 2010). However, because CloudSat data were not available, we determined the ice crystal number density (f) from the ice water content (c) following Sourdeval et al. (2018), assuming their diameters are above  $5 \mu\text{m}$ . The photon mean free path is calculated based on the particle distribution provided by DARDAR cloud products (Sourdeval et al., 2018). Figures 2(c-f) show that the lower clouds on the left of the panels have a layer of low-density ice crystal hydrometeors above and that the cloud top of the main cloud at lower latitudes contain highly concentrated ice with photon mean free path  $\sim 3 \text{ m}$ . Note that CALIPSO cannot penetrate below optically thick clouds with optical thickness bigger than 5 (Mace & Zhang, 2014) due to the attenuation of lidar signal (see the gray region "Presence of liquid unknown" in Figure 2(d)).

The detailed information for all the detected blue corona discharges is shown in Table S1 in Supplemental Material. Examples of a slow (rise time  $> 30 \mu\text{s}$ ) and fast (rise time  $\leq 30 \mu\text{s}$ ) corona

discharge measured by the ASIM photometers are shown in Figure 3(a,c). They are pulses in the blue photometer with absent or weak emissions in the red. We can estimate the altitude of the discharges from the temporal profile of the blue photometer pulses with a light-scattering model where discharges are assumed to be thin, straight, and uniformly bright segment inside a homogeneous cloud, emitting all photons at the same instance of time (Soler et al., 2020; Luque et al., 2020). The photons are scattered and absorbed by the hydrometeors, leading to broader pulses for sources deeper in the clouds. The model requires estimates of the photon mean free path  $\Lambda$  and number density  $n$ , but these parameters are usually not well known. Past reports assume the mean particle radius  $r = 10\text{--}20\text{ }\mu\text{m}$  and its density  $n = 1\text{--}2.5 \times 10^8\text{ m}^{-3}$  with the photon mean free path  $\Lambda = 1\text{--}20\text{ m}$  (Soler et al., 2020; Luque et al., 2020; Li et al., 2021; Li, Luque, Lehtinen, et al., 2022; Heumesser et al., 2021; Husbjerg et al., 2022). Because of the extraordinary luck with the CALIPSO observations, we can use measured parameters when modeling the discharges in the cloud of region  $\beta$ . Figures 2(e,f) indicate that most of the corona discharges are associated with  $\Lambda \sim 3\text{ m}$  and  $n \sim 5 \times 10^7\text{ m}^{-3}$ . In the fitting process, we select discharges with a clear impulsive single pulse and accept the fit when the coefficient of determination  $R^2 > 0.6$  (Chicco et al., 2021). Relying only on the coefficient of determination is not sufficient to exclude some multiple-pulse events (Li, Luque, Lehtinen, et al., 2022). Since the residual for a good fit is uncorrelated, approximately white noise, we exclude cases where the Pearson correlation coefficient ( $\rho$ ) between consecutive data points is larger than 0.5 (Magnello, 2009). Amongst the 92 corona discharges, 64 fulfill these conditions (See Table 1 in Supplemental Material) including 9 fast discharges and 55 slow discharges. The fit to the pulses in Figures 3(a,c) are shown as black solid lines. The depth in the cloud of the discharge are  $L = 2.06\text{ km}$  and  $0.45\text{ km}$ , respectively. The altitude in the cloud of the 28 corona discharges in region  $\beta$  is shown in Figure 2.

We explored if the discharges were associated with NBEs, as found in past studies, by searching the ENTLN data with a machine learning algorithm proposed by Zhu et al. (2021). We further required them to last for  $5\text{--}50\text{ }\mu\text{s}$  with clear ground waves and reflected sky waves. By identifying the polarity manually, we found 12 +NBEs (1 fast discharge and 11 slow discharges) and 3 -NBEs (1 fast discharge and 2 slow discharges), all correlated with the corona discharges observed by ASIM. Figures 3(b,d) show the ENTLN data of NBEs associated with the discharges of panels (a) and (c). The 9 discharges with NBEs that were found in region  $\beta$  are marked in Figure 2(b). Of the 28 discharges observed in region  $\beta$ , 5 were fast discharges close to the cloud top and 23 slow discharges deep inside the cloud. Although the data suggest a higher association of -NBE with fast rise times compared to +NBEs, our numbers are too small to draw a definitive conclusion. For instance, one +NBE correlate with a fast discharge, and 6 +NBEs and 2 -NBEs are related to the slow discharges. In addition, some +NBE and -NBE are found near each other in height, possibly because the charge distribution of the cloud is complex because of the highly dynamic convection and strong wind shear inside the cell (Stolzenburg et al., 1998; Stolzenburg & Marshall, 2009).

## 4 Discussion

Recent studies indicated that corona discharges are favoured by stronger convection and higher cloud tops than normal lightning (Husbjerg et al., 2022). Since the observed amount of corona discharges is limited by the passing time of ASIM, we further investigate the correlation between corona discharges, NBEs and lightning discharges based on the measurements from ENTLN. Figure 4 shows the time evolution of lightning and NBEs in region  $\beta$  detected by ENTLN during 4 hours from 18:00:00 to 22:00:00 UTC. The TBB temperature at the center of region  $\beta$  provided by Himawari-8 satellite is also given in Figure 4 as a reference for the storm height and intensity with its movie presented in Supplemental Material. The localized cell in region  $\beta$  occurred around 19:00 UTC associated with a small increase of the activity of both lightning and NBEs at 19:30 UTC, then it started to grow and spread out with both lightning discharges and NBEs increased dramatically and peaked at 20:10 UTC when ASIM passed over (gray rectangle region in Figure 4); finally, it dissipated around 20:40 UTC with another nearby cell at the left corner of region  $\beta$  starting to develop and move out of the region (see the small peak of TBB temperature at 21:10 UTC). Both +NBEs and -NBEs are correlated with an increase of lightning and with a decrease of the TBB temperature. As found in previous studies, this rapid increase of lightning frequency (termed “lightning jumps”



(Schultz et al., 2009)) is a good indicator of tropical storm intensity (Price et al., 2009; Lyons & Keen, 1994; Zipser & Lutz, 1994). According to Figure 4, both NBEs and corona discharges are found to be consistent with the evolution of the lightning activity (Chanrion et al., 2017).

Most often, fast discharges at cloud tops associate with -NBEs at the top edge of clouds (Soler et al., 2020; F. Liu, Lu, et al., 2021) and slow discharges related to +NBEs deeper in the clouds (Li et al., 2021; F. Liu, Lu, et al., 2021). Whereas the examples in Figure 3 appear to agree with this trend, we note that 12 +NBEs are associated with 1 fast discharges and 11 slow discharges and 3 -NBEs are related to 1 fast discharge and 2 slow discharges due to the complex charge distribution caused by severe convection and wind shear. However, the numbers in our case are too small to draw a definitive conclusion.

Only 20% of the corona discharges are associated with NBEs identified from the radio signals measured by ENTLN. It is unclear whether the NBE events are missed by ENTLN due to their weak amplitudes, complex wave-forms, or, as mentioned in previous studies, if some of them are related to an unknown process emitting weak, extremely short VHF pulses, named initial events (IEs) or the electromagnetic activities before the initial breakdown pulses (IBPs) (e.g., Marshall et al., 2019; Kostinskiy et al., 2020; Lyu et al., 2019) or they are associated with strong optical features but barely (or not at all) visible in radio signals, possibly because of their orientation (Li, Luque, Lehtinen, et al., 2022).

Similar to lightning, corona discharges seem to be generated nearby convective cloud “core” where deep convection lifts cloud droplets to high altitudes with a mixture of super-cooled cloud droplets, graupel, and ice crystals leading to electrification (Berdeklis & List, 2001; Dimitriadou et al., 2022). Most of the discharges are located close to high ice water content giving a photon mean free path  $\Lambda \approx 3$  m which is consistent with previous studies that assumed the particle sizes and the densities with the photon mean free path ranging from  $\sim 1$ -20 m (Soler et al., 2020; Li et al., 2021; Li, Luque, Lehtinen, et al., 2022; Luque et al., 2020; Heumesser et al., 2021; Husbjerg et al., 2022). Future studies should address the role of a non-uniform particle distribution inside a cloud and assess the validity of the approximations employed here.

## Acknowledgments

This work was supported by Independent Research Fund Denmark (Danmarks Frie Forskningsfond) under grant agreement 1026-00420B. The project has received funding from the European Union’s Horizon 2020 research and innovation program under the Marie Skłodowska-Curie grant agreement SAINT 722337.

## Open Research

The Modular Multispectral Imaging Array (MMIA) level 1 data is proprietary and not currently available for public release. Interested parties should direct their request to the ASIM Facility Science Team (FST). ASIM data request can be submitted through: <https://asdc.space.dtu.dk> by sending a message to the electronic address [asdc@space.dtu.dk](mailto:asdc@space.dtu.dk). The Himawari-8 gridded products are public to the registered users and supplied by the P-Tree System, Japan Aerospace Exploration Agency (JAXA)/Earth Observation Research Center (EORC) (<https://www.eorc.jaxa.jp/ptree/>). Earth Networks Total Lightning Network (ENTLN) products can be obtained from <https://www.earthnetworks.com/why-us/networks/lightning/> by contacting Earth Networks team through [info@earthnetworks.com](mailto:info@earthnetworks.com). The raDAR/liDAR (DARDAR) cloud products are public to the registered users at <https://www.icare.univ-lille.fr/dardar/overview-dardar-nice/>. CALIPSO data products are public to the registered users at <https://www-calipso.larc.nasa.gov/>. ERA5 hourly reanalysis data are public to the registered users, for the single level data can be found at <https://cds.climate.copernicus.eu/cdsapp#!/dataset/reanalysis-era5-single-levels?tab=overview>, for the pressure levels data can be obtained at <https://cds.climate.copernicus.eu/cdsapp#!/dataset/reanalysis-era5-pressure-levels?tab=overview>. NRT Lightning Imaging Sensor (LIS) on International Space

Station (ISS) Science Data V2 is public to the registered users and is available at <https://search.earthdata.nasa.gov/search?q=isslis.v2.nrt>.

## References

- Berdeklis, P., & List, R. (2001). The Ice Crystal–Graupel Collision Charging Mechanism of Thunderstorm Electrification. *Journal of the Atmospheric Sciences*, 58(18), 2751–2770. doi: 10.1175/1520-0469(2001)058<2751:TICGCC>2.0.CO;2
- Bessho, K., DATE, K., HAYASHI, M., IKEDA, A., IMAI, T., INOUE, H., ... YOSHIDA, R. (2016). An introduction to himawari-8/9—japan’s new-generation geostationary meteorological satellites. *Journal of the Meteorological Society of Japan. Ser. II*, 94(2), 151–183. doi: 10.2151/jmsj.2016-009
- Bitzer, P. M., Walker, T. D., Lang, T. J., Gatlin, P. N., Chanrion, O., Neubert, T., ... Victor, R. (2021). Multifrequency optical observations of lightning with ISS-LIS and ASIM. In *AGU Fall Meeting 2021*.
- Blakeslee, R. J., Lang, T. J., Koshak, W. J., Buechler, D., Gatlin, P., Mach, D. M., ... Christian, H. (2020). Three Years of the Lightning Imaging Sensor Onboard the International Space Station: Expanded Global Coverage and Enhanced Applications. *Journal of Geophysical Research: Atmospheres*, 125(16), e2020JD032918. doi: <https://doi.org/10.1029/2020JD032918>
- Chanrion, O., Neubert, T., Mogensen, A., Yair, Y., Stendel, M., Singh, R., & Siingh, D. (2017). Profuse activity of blue electrical discharges at the tops of thunderstorms. *Geophysical Research Letters*, 44(1), 496–503. doi: <https://doi.org/10.1002/2016GL071311>
- Chanrion, O., Neubert, T., Rasmussen, I. L., Stoltze, C., Tcherniak, D., Jessen, N. C., ... others (2019). The Modular Multispectral Imaging Array (MMIA) of the ASIM payload on the international space station. *Space Science Reviews*, 215(4), 1–25. doi: <https://doi.org/10.1007/s11214-019-0593-y>
- Chauhan, A., Singh, R. P., Dash, P., & Kumar, R. (2021). Impact of tropical cyclone “Fani” on land, ocean, atmospheric and meteorological parameters. *Marine Pollution Bulletin*, 162, 111844. doi: <https://doi.org/10.1016/j.marpolbul.2020.111844>
- Chicco, D., Warrens, M. J., & Jurman, G. (2021). The coefficient of determination R-squared is more informative than SMAPE, MAE, MAPE, MSE and RMSE in regression analysis evaluation. *PeerJ Computer Science*, 7, e623. doi: <https://doi.org/10.7717/peerj-cs.623>
- Chou, J. K., Hsu, R.-R., Su, H.-T., Chen, A. B.-C., Kuo, C.-L., Huang, S.-M., ... Wu, Y.-J. (2018). ISUAL-Observed Blue Luminous Events: The Associated Sferics. *Journal of Geophysical Research: Space Physics*, 123(4), 3063–3077. doi: <https://doi.org/10.1002/2017JA024793>
- Christian, H. J., Blakeslee, R. J., & Goodman, S. J. (1989). The detection of lightning from geostationary orbit. *Journal of Geophysical Research: Atmospheres*, 94(D11), 13329–13337. doi: <https://doi.org/10.1029/JD094iD11p13329>
- da Silva, C. L., & Pasko, V. P. (2013). Dynamics of streamer-to-leader transition at reduced air densities and its implications for propagation of lightning leaders and gigantic jets. *Journal of Geophysical Research: Atmospheres*, 118(24), 13,561–13,590. doi: <https://doi.org/10.1002/2013JD020618>
- Delanoë, J., & Hogan, R. J. (2010). Combined CloudSat–CALIPSO–MODIS retrievals of the properties of ice clouds. *Journal of Geophysical Research: Atmospheres*, 115(D4). doi: <https://doi.org/10.1029/2009JD012346>
- Dimitriadou, K., Chanrion, O., Neubert, T., Protat, A., Louf, V., Heumesser, M., ... Reglero, V. (2022). Analysis of Blue Corona Discharges at the Top of Tropical Thunderstorm Clouds in Different Phases of Convection. *Geophysical Research Letters*, 49(6), e2021GL095879. doi: <https://doi.org/10.1029/2021GL095879>
- Ebert, U., & Sentman, D. D. (2008, nov). Streamers, sprites, leaders, lightning: from micro- to macroscales. *Journal of Physics D: Applied Physics*, 41(23), 230301. doi: 10.1088/0022-3727/41/23/230301
- Goodman, S. J., Blakeslee, R. J., Koshak, W. J., Mach, D., Bailey, J., Buechler, D., ... Stano, G. (2013). The goes-r geostationary lightning mapper (glm). *Atmospheric Research*, 125–126,

- 34-49.
- Gordillo-Vázquez, F., & Pérez-Invernón, F. (2021). A review of the impact of transient luminous events on the atmospheric chemistry: Past, present, and future. *Atmospheric Research*, 252, 105432. Retrieved from <https://www.sciencedirect.com/science/article/pii/S0169809520313697> doi: <https://doi.org/10.1016/j.atmosres.2020.105432>
- Grandell, J., Stuhlmann, R., Dobber, M., Bennett, A., Biron, D., Defer, E., ... Mtg Lightning Imager Science Team (2010, December). EUMETSAT Meteosat Third Generation (MTG) Lightning Imager: From mission requirements to product development. In *Agu fall meeting abstracts* (Vol. 2010, p. AE21A-0257).
- Gryspeerd, E., Sourdeval, O., Quaas, J., Delanoë, J., Krämer, M., & Kühne, P. (2018). Ice crystal number concentration estimates from lidar-radar satellite remote sensing – Part 2: Controls on the ice crystal number concentration. *Atmospheric Chemistry and Physics*, 18(19), 14351–14370. Retrieved from <https://acp.copernicus.org/articles/18/14351/2018/> doi: 10.5194/acp-18-14351-2018
- Hagihara, Y., Okamoto, H., & Luo, Z. J. (2014). Joint analysis of cloud top heights from CloudSat and CALIPSO: New insights into cloud top microphysics. *Journal of Geophysical Research: Atmospheres*, 119(7), 4087–4106. doi: <https://doi.org/10.1002/2013JD020919>
- Hersbach, H., Bell, B., Berrisford, P., Hirahara, S., Horányi, A., Muñoz-Sabater, J., ... Thépaut, J.-N. (2020). The era5 global reanalysis. *Quarterly Journal of the Royal Meteorological Society*, 146(730), 1999–2049. doi: <https://doi.org/10.1002/qj.3803>
- Heumesser, M., Chanrion, O., Neubert, T., Christian, H. J., Dimitriadou, K., Gordillo-Vazquez, F. J., ... Köhn, C. (2021). Spectral Observations of Optical Emissions Associated With Terrestrial Gamma-Ray Flashes. *Geophysical Research Letters*, 48(4), 2020GL090700. doi: <https://doi.org/10.1029/2020GL090700>
- Husbjerg, L. S., Neubert, T., Chanrion, O., Dimitriadou, K., Li, D., Stendel, M., ... Reglero, V. (2022). Observations of Blue Corona Discharges in Thunderclouds. *Geophysical Research Letters*, 49(12), e2022GL099064. doi: <https://doi.org/10.1029/2022GL099064>
- Kostinskiy, A. Y., Marshall, T. C., & Stolzenburg, M. (2020). The Mechanism of the Origin and Development of Lightning From Initiating Event to Initial Breakdown Pulses (v.2). *Journal of Geophysical Research: Atmospheres*, 125(22), e2020JD033191. doi: 10.1029/2020JD033191
- Li, D., Luque, A., Gordillo-Vázquez, F. J., Liu, F., Lu, G., Neubert, T., ... Reglero, V. (2021). Blue Flashes as Counterparts to Narrow Bipolar Events: The Optical Signal of Shallow In-Cloud Discharges. *Journal of Geophysical Research: Atmospheres*, 126(13), e2021JD035013. doi: 10.1029/2021JD035013
- Li, D., Luque, A., Gordillo-Vázquez, F. J., Silva, C. d., Krehbiel, P. R., Rachidi, F., & Rubinstein, M. (2022). Secondary Fast Breakdown in Narrow Bipolar Events. *Geophysical Research Letters*, 49(7), e2021GL097452. (e2021GL097452 2021GL097452) doi: <https://doi.org/10.1029/2021GL097452>
- Li, D., Luque, A., Lehtinen, N. G., Gordillo-Vázquez, F. J., Neubert, T., Lu, G., ... Reglero, V. (2022). Multi-pulse corona discharges in thunderclouds observed in optical and radio bands. *Geophysical Research Letters*, e2022GL098938. doi: <https://doi.org/10.1029/2022GL098938>
- Lidar Level 1 V4.10 Data Product Descriptions. (2016). [https://www-calipso.larc.nasa.gov/resources/calipso.users.guide/data\\_summaries/l1b/index\\_v4-x.php#tropopause.height](https://www-calipso.larc.nasa.gov/resources/calipso.users.guide/data_summaries/l1b/index_v4-x.php#tropopause.height). ([Online; accessed 30-June-2022])
- Liu, F., Lu, G., Neubert, T., Lei, J., Chanrion, O., Østgaard, N., ... Zhu, B. (2021). Optical emissions associated with narrow bipolar events from thunderstorm clouds penetrating into the stratosphere. *Nature Communications*, 12(6631). doi: <https://doi.org/10.1038/s41467-021-26914-4>
- Liu, F., Zhu, B., Lu, G., Lei, J., Shao, J., Chen, Y., ... Zhou, H. (2021). Meteorological and Electrical Conditions of Two Mid-latitude Thunderstorms Producing Blue Discharges. *Journal of Geophysical Research: Atmospheres*, 126(8), e2020JD033648. doi: <https://doi.org/10.1029/2020JD033648>
- Liu, F., Zhu, B., Lu, G., Qin, Z., Lei, J., Peng, K.-M., ... Zhou, H. (2018). Observations of Blue Discharges Associated With Negative Narrow Bipolar Events in Active Deep Convection. *Geophysical Research Letters*, 45(6), 2842–2851. doi: <https://doi.org/10.1002/2017GL076207>



- Liu, N., Dwyer, J. R., Tilles, J. N., Stanley, M. A., Krehbiel, P. R., Rison, W., ... Wilson, J. G. (2019). Understanding the Radio Spectrum of Thunderstorm Narrow Bipolar Events. *Journal of Geophysical Research: Atmospheres*, 124(17-18), 10134-10153. doi: <https://doi.org/10.1029/2019JD030439>
- Liu, Z., Vaughan, M., Winker, D., Kittaka, C., Getzewich, B., Kuehn, R., ... Hostetler, C. (2009). The calipso lidar cloud and aerosol discrimination: Version 2 algorithm and initial assessment of performance. *Journal of Atmospheric and Oceanic Technology*, 26(7), 1198 - 1213. doi: 10.1175/2009JTECHA1229.1
- Luque, A., Gordillo-Vázquez, F. J., Li, D., Malagón-Romero, A., Pérez-Invernón, F. J., Schmalzried, A., ... Østgaard, N. (2020). Modeling lightning observations from space-based platforms (CloudScat.jl 1.0). *Geoscientific Model Development*, 13(11), 5549-5566. doi: <https://doi.org/10.5194/gmd-13-5549-2020>
- Lyons, W. A., & Keen, C. S. (1994). Observations of Lightning in Convective Supercells within Tropical Storms and Hurricanes. *Monthly Weather Review*, 122(8), 1897 - 1916. doi: 10.1175/1520-0493(1994)122<1897:OOLICS>2.0.CO;2
- Lyons, W. A., Nelson, T. E., Armstrong, R. A., Pasko, V. P., & Stanley, M. A. (2003). Upward electrical discharges from thunderstorm tops. *Bulletin of the American Meteorological Society*, 84(4), 445-454.
- Lyu, F., Cummer, S. A., Qin, Z., & Chen, M. (2019). Lightning Initiation Processes Imaged With Very High Frequency Broadband Interferometry. *Journal of Geophysical Research: Atmospheres*, 124(6), 2994-3004. doi: <https://doi.org/10.1029/2018JD029817>
- Mace, G. G., & Zhang, Q. (2014). The CloudSat radar-lidar geometrical profile product (RL-GeoProf): Updates, improvements, and selected results. *Journal of Geophysical Research: Atmospheres*, 119(15), 9441-9462. doi: <https://doi.org/10.1002/2013JD021374>
- Magnello, M. E. (2009). Karl Pearson and the Establishment of Mathematical Statistics. *International Statistical Review*, 77(1), 3-29. doi: <https://doi.org/10.1111/j.1751-5823.2009.00073.x>
- Marshall, T., Bandara, S., Karunarathne, N., Karunarathne, S., Kolmasova, I., Siedlecki, R., & Stolzenburg, M. (2019). A study of lightning flash initiation prior to the first initial breakdown pulse. *Atmospheric Research*, 217, 10-23. doi: 10.1016/j.atmosres.2018.10.013
- Montanyà, J., López, J. A., Morales Rodriguez, C. A., van der Velde, O. A., Fabró, F., Pineda, N., ... Freijó, M. (2021). A Simultaneous Observation of Lightning by ASIM, Colombia-Lightning Mapping Array, GLM, and ISS-LIS. *Journal of Geophysical Research: Atmospheres*, 126(6), e2020JD033735. doi: <https://doi.org/10.1029/2020JD033735>
- Neubert, T., Chanrion, O., Heumesser, M., Dimitriadou, K., Husbjerg, L., Rasmussen, I. L., ... Reglero, V. (2021). Observation of the onset of a blue jet into the stratosphere. *Nature*, 589(7842), 371-375. doi: <https://doi.org/10.1038/s41586-020-03122-6>
- Neubert, T., Østgaard, N., Reglero, V., Blanc, E., Chanrion, O., Oxborrow, C. A., ... Bhandari, D. D. (2019). The ASIM mission on the international space station. *Space Science Reviews*, 215(2), 1-17. doi: <https://doi.org/10.1007/s11214-019-0592-z>
- O'Neill, M. E., Orf, L., Heymsfield, G. M., & Halbert, K. (2021). Hydraulic jump dynamics above supercell thunderstorms. *Science*, 373(6560), 1248-1251. doi: 10.1126/science.abh3857
- Pasko, V. P. (2008, nov). Blue jets and gigantic jets: transient luminous events between thunderstorm tops and the lower ionosphere. *Plasma Physics and Controlled Fusion*, 50(12), 124050. doi: <https://doi.org/10.1088/0741-3335/50/12/124050>
- Price, C., Asfur, M., & Yair, Y. (2009). Maximum hurricane intensity preceded by increase in lightning frequency. *Nature Geoscience*, 2(5), 329-332. doi: <https://doi.org/10.1038/ngeo477>
- Pucik, T., Groenemeijer, P., & Tsonevsky, I. (2021, 01). Vertical wind shear and convective storms. (879). Retrieved from <https://www.ecmwf.int/node/19905> doi: 10.21957/z0b3t5mrv
- Raizer, Y. P., & Allen, J. E. (1991). *Gas discharge physics* (Vol. 1). Springer.
- Rison, W., Krehbiel, P. R., Stock, M. G., Edens, H. E., Shao, X.-M., Thomas, R. J., ... Zhang, Y. (2016). Observations of narrow bipolar events reveal how lightning is initiated in thunderstorms. *Nature communications*, 7, 10721. doi: 10.1038/ncomms10721(2016)
- Schultz, C. J., Petersen, W. A., & Carey, L. D. (2009). Preliminary development and evaluation of lightning jump algorithms for the real-time detection of severe weather. *Journal of Applied*

- Meteorology and Climatology*, 48(12), 2543–2563. doi: <https://doi.org/10.1175/2009JAMC2237.1>
- Smith, D. A., Heavner, M. J., Jacobson, A. R., Shao, X. M., Massey, R. S., Sheldon, R. J., & Wiens, K. C. (2004). A method for determining intracloud lightning and ionospheric heights from VLF/LF electric field records. *Radio Science*, 39(1), RS1010. doi: <https://doi.org/10.1029/2002RS002790>
- Smith, D. A., Shao, X. M., Holden, D. N., Rhodes, C. T., Brook, M., Krehbiel, P. R., ... Thomas, R. J. (1999). A distinct class of isolated intracloud lightning discharges and their associated radio emissions. *Journal of Geophysical Research: Atmospheres*, 104(D4), 4189–4212. doi: <https://doi.org/10.1029/1998JD200045>
- Soler, S., Gordillo-Vázquez, F. J., Pérez-Invernón, F. J., Luque, A., Li, D., Neubert, T., ... Østgaard, N. (2021). Global Frequency and Geographical Distribution of Nighttime Streamer Corona Discharges (BLUEs) in Thunderclouds. *Geophysical Research Letters*, 48(18), e2021GL094657. doi: <https://doi.org/10.1029/2021GL094657>
- Soler, S., Pérez-Invernón, F. J., Gordillo-Vázquez, F. J., Luque, A., Li, D., Malagón-Romero, A., ... Østgaard, N. (2020). Blue Optical Observations of Narrow Bipolar Events by ASIM Suggest Corona Streamer Activity in Thunderstorms. *Journal of Geophysical Research: Atmospheres*, 125(16), e2020JD032708. doi: [10.1029/2020JD032708](https://doi.org/10.1029/2020JD032708)
- Sourdeval, O., Gryspeerdt, E., Krämer, M., Goren, T., Delanoë, J., Afchine, A., ... Quaas, J. (2018). Ice crystal number concentration estimates from lidar–radar satellite remote sensing – Part 1: Method and evaluation. *Atmospheric Chemistry and Physics*, 18(19), 14327–14350. Retrieved from <https://acp.copernicus.org/articles/18/14327/2018/> doi: [10.5194/acp-18-14327-2018](https://doi.org/10.5194/acp-18-14327-2018)
- Stolzenburg, M., & Marshall, T. C. (2009). Electric Field and Charge Structure in Lightning-Producing Clouds. In H. D. Betz, U. Schumann, & P. Laroche (Eds.), *Lightning: Principles, instruments and applications: Review of modern lightning research* (pp. 57–82). Dordrecht: Springer Netherlands. doi: [10.1007/978-1-4020-9079-0\\_3](https://doi.org/10.1007/978-1-4020-9079-0_3)
- Stolzenburg, M., Rust, W. D., & Marshall, T. C. (1998). Electrical structure in thunderstorm convective regions: 3. Synthesis. *Journal of Geophysical Research: Atmospheres*, 103(D12), 14097–14108. doi: <https://doi.org/10.1029/97JD03545>
- Tilles, J. N., Liu, N., Stanley, M. A., Krehbiel, P. R., Rison, W., Stock, M. G., ... Wilson, J. (2019). Fast negative breakdown in thunderstorms. *Nature communications*, 10(1), 1–12.
- Walker, T. D., & Christian, H. J. (2019). Triggered lightning spectroscopy: 2. a quantitative analysis. *Journal of Geophysical Research: Atmospheres*, 124(7), 3930–3942. doi: <https://doi.org/10.1029/2018JD029901>
- Wang, P. K., Cheng, K.-Y., Setvak, M., & Wang, C.-K. (2016). The origin of the gullwing-shaped cirrus above an Argentinian thunderstorm as seen in CALIPSO images. *Journal of Geophysical Research: Atmospheres*, 121(7), 3729–3738. doi: <https://doi.org/10.1002/2015JD024111>
- Wescott, E. M., Sentman, D. D., Heavner, M. J., Hampton, D. L., Osborne, D. L., & Vaughan Jr., O. H. (1996). Blue starters Brief upward discharges from an intense Arkansas thunderstorm. *Geophysical Research Letters*, 23(16), 2153–2156. doi: <https://doi.org/10.1029/96GL01969>
- Wescott, E. M., Sentman, D. D., Stenbaek-Nielsen, H. C., Huet, P., Heavner, M. J., & Moudry, D. R. (2001). New evidence for the brightness and ionization of blue starters and blue jets. *Journal of Geophysical Research: Space Physics*, 106(A10), 21549–21554. doi: <https://doi.org/10.1029/2000JA000429>
- Winker, D., Pelon, J., Coakley Jr, J., Ackerman, S., Charlson, R., Colarco, P., ... others (2010). The CALIPSO mission: A global 3D view of aerosols and clouds. *Bulletin of the American Meteorological Society*, 91(9), 1211–1230. doi: <https://doi.org/10.1175/2010BAMS3009.1>
- Wu, T., Dong, W., Zhang, Y., Funaki, T., Yoshida, S., Morimoto, T., ... Kawasaki, Z. (2012). Discharge height of lightning narrow bipolar events. *Journal of Geophysical Research: Atmospheres*, 117(D5). doi: <https://doi.org/10.1029/2011JD017054>
- Yang, J., Zhang, Z., Wei, C., Lu, F., & Guo, Q. (2017). Introducing the new generation of Chinese geostationary weather satellites, Fengyun-4. *Bulletin of the American Meteorological Society*, 98(8), 1637–1658. doi: <https://doi.org/10.1175/BAMS-D-16-0065.1>

- 484 Zhao, L., Wang, S.-Y. S., Becker, E., Yoon, J.-H., & Mukherjee, A. (2020, aug). Cyclone Fani: the  
485 tug-of-war between regional warming and anthropogenic aerosol effects. *Environmental Research*  
486 *Letters*, 15(9), 094020. Retrieved from <https://doi.org/10.1088/1748-9326/ab91e7> doi:  
487 10.1088/1748-9326/ab91e7
- 488 Zhu, Y., Bitzer, P., Rakov, V., & Ding, Z. (2021). A Machine-Learning Approach to Classify Cloud-  
489 to-Ground and Intracloud Lightning. *Geophysical Research Letters*, 48(1), e2020GL091148.  
490 (e2020GL091148 2020GL091148) doi: <https://doi.org/10.1029/2020GL091148>
- 491 Zhu, Y., Rakov, V. A., Tran, M. D., Stock, M. G., Heckman, S., Liu, C., ... Hare, B. M. (2017).  
492 Evaluation of ENTLN Performance Characteristics Based on the Ground Truth Natural and  
493 Rocket-Triggered Lightning Data Acquired in Florida. *Journal of Geophysical Research: At-*  
494 *mospheres*, 122(18), 9858-9866. doi: <https://doi.org/10.1002/2017JD027270>
- 495 Zhu, Y., Stock, M., Lapierre, J., & DiGangi, E. (2022). Upgrades of the earth networks total  
496 lightning network in 2021. *Remote Sensing*, 14(9). doi: 10.3390/rs14092209
- 497 Zipser, E. J., & Lutz, K. R. (1994). The Vertical Profile of Radar Reflectivity of Convective Cells: A  
498 Strong Indicator of Storm Intensity and Lightning Probability? *Monthly Weather Review*, 122(8),  
499 1751 - 1759. doi: 10.1175/1520-0493(1994)122<1751:TVPORR>2.0.CO;2

500

# Figure list

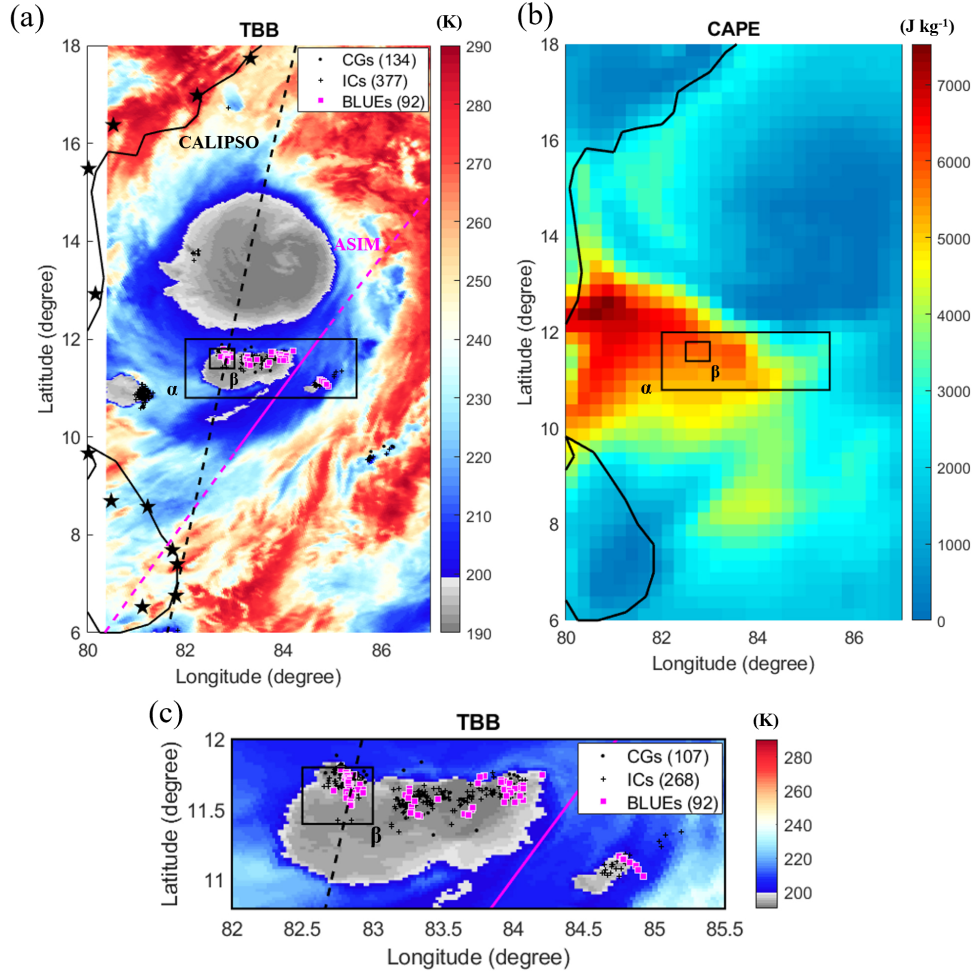


**Figure 1.** The distribution of CG (black dots)/IC (black cross) lightning activity and corona discharges (pink square) activity superimposed on TBB temperature (K) provided by the Himawari-8 satellite at 20:10:00 UTC (a), Convective Available Potential Energy (CAPE) (b) based on ERA5 hourly reanalysis data at 20:00:00 UTC, and (c) the zoom of region  $\alpha$  in (a). The footprints of ASIM and CALIPSO are shown as pink and black dashed lines, respectively. The ground-based ENTLN sensors are shown as black stars. The region  $\beta$  in (a,b,c) is observed by both ASIM and CALIPSO within 12 minutes.

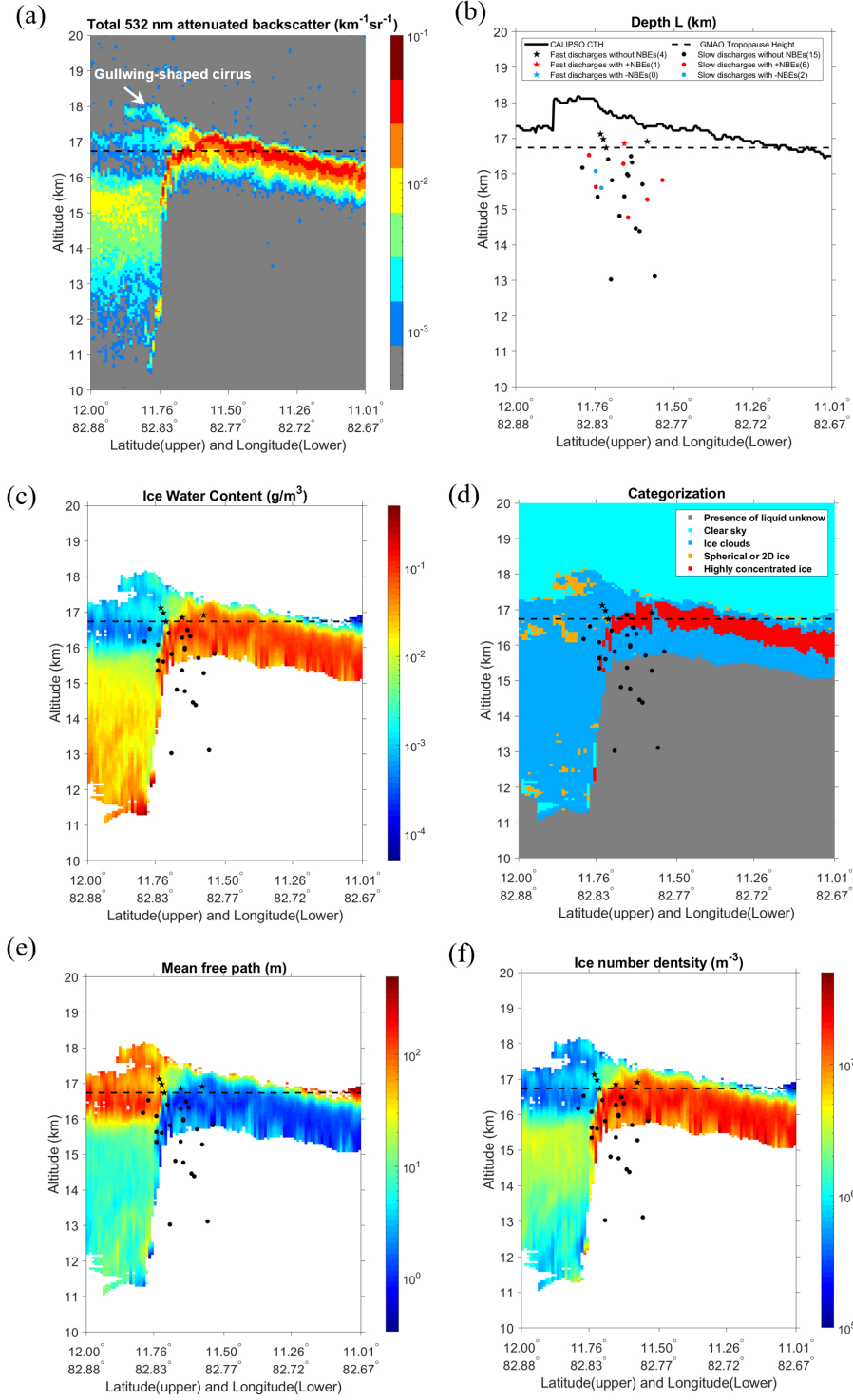


**Figure 2.** (a) A cross section of 532 nm lidar backscattering coefficient profile obtained along the trajectory of CALIPSO in region  $\beta$  (black dashed line in Figure 1(c)), (b) the depth of corona discharges in region  $\beta$  relative to the inferred CTH based on CALIPSO lidar backscattering coefficient profile in (a). The distribution of cloud microphysical properties based on the DARDAR cloud products including (c) Ice water content, (d) Categorization, (e) Photon mean free path and (f) Ice crystal number density. Fast and slow discharges are the closest events in the CALIPSO trajectory, shown in star and dot shape, respectively. Tropopause height is shown by black dashed line. The gullwing-shaped cirrus (marked by white arrows in (a)) higher than the overshooting top shows a clear indication for the convective transport between the troposphere and the stratosphere.



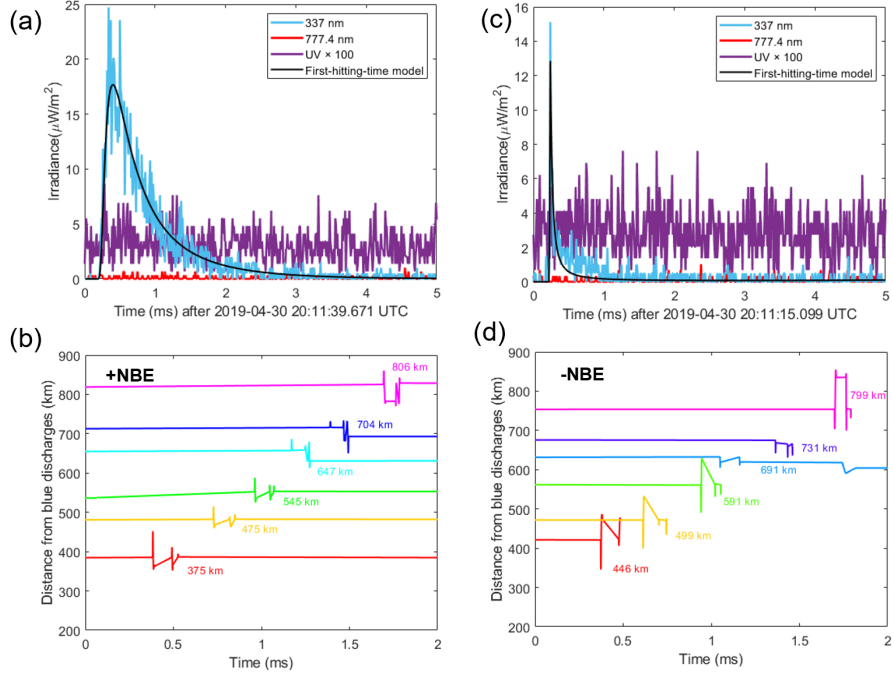


**Figure 3.** Examples of a slow corona discharge (a) and a fast corona discharge (c) associated with +NBE (b) and -NBE (d) observed by different ENTLN sensors located at different observation distances, respectively. (a,c) MMIA photometer irradiance (blue: 337 nm, purple: 180-230 nm ( $UV \times 100$ ), red: 777.4 nm and black: modeling result of the first-hitting-time model with the depth  $L = 2.06$  km (a) and 0.45 km (c), respectively) and (b,d) the corresponding radio signal detected from the ground-based electric field sensors from ENTLN. The time in (b,d) is the detected time of different electric field sensors.

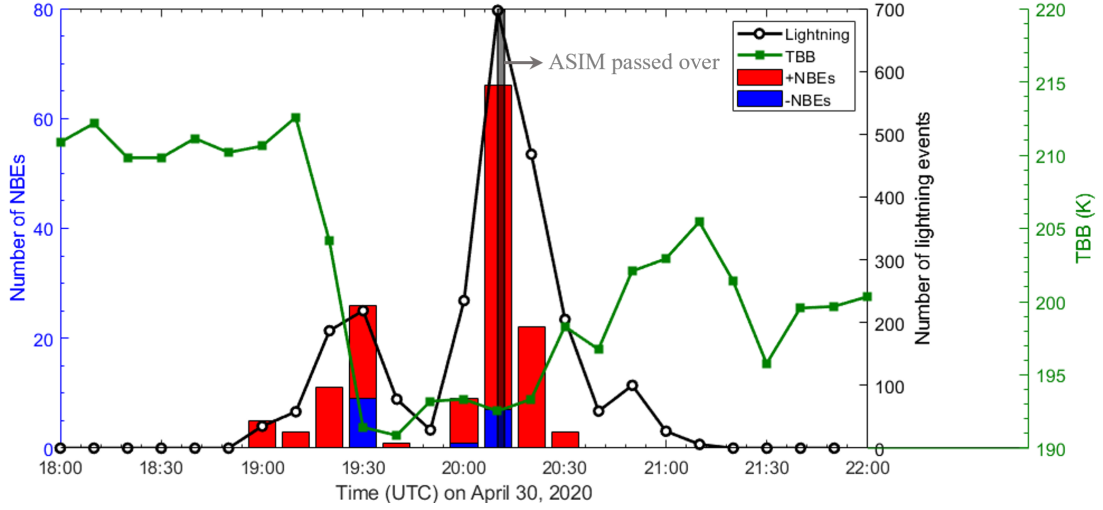


**Figure 4.** The time evolution of lightning (black) and NBEs (+NBE (red) and -NBE (blue) ) in region  $\beta$  detected by ENTLN along with TBB temperature (green) at the center of region  $\beta$  provided by Himawari-8 satellite during the time period from 18:00:00 to 22:00:00 UTC. The occurred time period of 92 corona discharges detected by ASIM is marked by gray rectangle.